Conference on Modelling Fluid Flow (CMFF'25)
The 19th International Conference on Fluid Flow Technologies
Budapest, Hungary, August 26-August 29, 2025

The Effect of Housing Recess Geometry on Fiber Entry into the Back Shroud Cavity of a Wastewater Pump

Tobias RINNERT[1], Paul Uwe THAMSEN[2],

[1] Corresponding Author. Department of Fluid System Dynamics, Faculty of Mechanical Engineering and Transport Systems, Technische Universität Berlin. Straße des 17. Juni 135, 10623 Berlin, Germany. Tel.: +49 30 314 70930, E-mail: t.rinnert@tu-berlin.de
[2] Department of Fluid System Dynamics, Faculty of Mechanical Engineering and Transport Systems, Technische Universität Berlin. Straße des 17. Juni 135, 10623 Berlin, Germany. Tel.: +49 30 314 25262, E-mail: paul-uwe.thamsen@tu-berlin.de

ABSTRACT

In this paper, the influence of several housing recess geometries on the fiber entry into the back shroud cavity of a single volute wastewater pump with a semi-open two-channel impeller is investigated. The test rig used is a wastewater pumping station model that provides optical access into areas in wastewater pumps that are at risk of clogging. Three operating points are examined for each configuration, one at part load, one at best efficiency point and one at overload. The introduced configurations feature varying radial gap widths between back shroud and outer diameter of the recess as well as different degrees of back shroud coverage. The axial gap width between recessed rear housing wall and flat disk back shroud corresponds to 5 *mm*. Tested configurations are evaluated on the basis of dry fiber mass permanently accumulated in the back shroud cavity after pumping artificial wastewater for 60 *min*. The evaluation of the experimental data shows that housing recesses with partial or complete back shroud coverage significantly reduce or completely eliminate fiber entry while increasing efficiency.

Keywords: back shroud cavity, clogging, fibers, housing recess, wastewater pump

NOMENCLATURE

H	$[m]$	head
N_S	$[min^{-1}]$	specific speed (US customary)
P	$[W]$	power
Q	$[m^3 s^{-1}]$	flow rate
R	$[mm]$	radius
Re	[-]	Reynolds number
S	[-]	gap ratio
T	$[min]$	time
c	[-]	degree of coverage
d	$[mm]$	depth
g	$[ms^{-2}]$	gravitational acceleration
n_q	$[min^{-1}]$	specific speed (metric)
s	$[mm]$	gap width
t	$[mm]$	thickness
η	[-]	efficiency
ρ	$[kgm^{-3}]$	mass density

Subscripts and Superscripts

BS	back shroud
HR	housing recess
a	aggregate
ax	axial
c	critical
el	electrical
$hydr$	hydraulic
r	radial

1. INTRODUCTION

Being part of critical infrastructure, wastewater pumps are expected to operate clogging-free, safely and efficiently [1, 2]. However, continuous entry of fibers from nonwoven wipes is one of major obstacles for the reliable operation of wastewater systems all over the world [3]. Although the yearly nonwoven wipe production throughout Europe has declined slightly since its all-time high of almost 3.25 million tons in 2021, in 2023 it was still 2.8 times the amount produced in 2000 [3, 4]. The fibers contained in the wastewater frequently accumulate in wastewater pumps at the blade inlet, on the cutwater and in the front and back shroud cavity [2, 5, 6]. In addition to the risk of clogging, fibers entering the back shroud cavity can pose a risk to the mechanical seal [7]. The *functionality*, i.e. the ability of a pump to transport fiber-laden wastewater without clogging [8], is therefore of utmost importance, as it may furthermore reduce the aforementioned requirements operational safety and efficiency [3, 9]. The only thing worse than an inefficiently operated wastewater pump is one that cannot be operated when needed. Cities such as London, New York and Sydney each bear annual resulting costs of tens of millions USD [3].

In order to meet the requirements discussed, there are numerous design guidelines available that vary depending on wastewater composition [10, 11]. In wastewater pumps, vortex as well as one-, two- and three-channel impellers are commonly in use [2]. When pumping large solids, clogging can be easily avoided by choosing wastewater impellers that feature a sufficiently large *ball passage* [5]. When it comes to pumping fiber-laden wastewater, however, the susceptibility to clogging is independent of the ball passage, as experimentally determined by Pöhler and Thamsen [12] for a wide variety of wastewater pump impellers. Wastewater pumps are usually designed as single-stage pumps with a volute or annular casing [2, 5]. This is due to the fact that the bladed guide vanes found in multistage pumps are prone to clogging [5, 10]. Furthermore, balance holes in the back shroud are avoided in wastewater pumps as well for the same reason, so that axial thrust reduction is typically achieved by back vanes [5].

However, only vague design guidelines are available to keep the back shroud cavity free of fibers or other solids. Housing recesses as well as back vanes are stated as solutions [5, 7, 13, 14]. In preliminary tests on the wastewater pump investigated in this paper, the fiber entry into the back shroud cavity was found to significantly decrease as the axial gap width s_{ax} between flat disk-shaped back shroud and rear housing wall decreases [15]. Further investigations on this wastewater pump focused on the influence of specific design parameters for backward curved back vanes and back channels on fiber entry into the back shroud cavity [16]. It showed, that backward curved back vanes can eliminate fiber entry into the back shroud completely even at low back vane height and with minor efficiency drawbacks. In contrast, only the one back channel configuration investigated at minimum axial gap width between the unmodified part of the back shroud and rear housing wall, as well as maximum channel depth, was found to be capable of slightly decreasing fiber entry at a disproportionate reduction in efficiency.

2. BACK SHROUD CAVITY FLOW

Hardly anything in a centrifugal pump has as powerful an influence on other essential components and operating behavior due to its design characteristics as the cavities between impeller and housing. The flow prevailing there not only largely defines axial thrust [5, 10]. It is furthermore well known, that the shroud cavity design may significantly affect radial thrust as well [5]. Besides axial thrust, the pressure within the back shroud cavity is also to be considered when choosing the shaft seal. With regard to pump efficiency, shroud cavity design impacts leakage losses and, in particular, disk friction losses [10, 17]. The latter is nothing less than the fundamental motivation for the experiments on disks rotating in cylindrical housings, as conducted by Schultz-Grunow [18], Ippen [19] or Daily and Nece [20, 21], from which the basic understanding of back shroud cavity flow is derived [5, 10].

2.1. Theory

Based on analytical and experimental investigations on *enclosed rotating disk flow* conducted by Daily and Nece [20, 21], it has become common practice to distinguish between the following four flow regimes, depending on the properties of disk and rear housing wall boundary layers:

I. merged, laminar
II. separated, laminar
III. merged, turbulent
IV. separated, turbulent

Reynolds number Re and axial gap width s_{ax} define the corresponding flow regime prevailing. However, surface roughness can increase boundary layer thickness and decrease the critical Reynolds number Re_c. [20, 21]

Within the disk boundary layer, the circumferential velocity is increased compared to the rest of the fluid. Directly on the rotating disk surface, the fluid moves with the local circumferential velocity of the disk itself, due to the no slip boundary condition. Accordingly, the no slip boundary condition causes the circumferential speed to be zero directly on the stationary rear housing surface. Compared to the rest of the fluid, the circumferential velocity is decreased within the rear housing boundary layer. Due to the increased circumferential speed within the rotating disk boundary layer, the fluid is therein centrifuged outward. Continuity enforces a radially inward directed flow within the housing wall boundary layer, which leads to the characteristic radial-axial circulation between disk and rear housing wall. Together with the explained circumferential velocity distribution, this yields the three-dimensional flow around enclosed rotating disks. For sufficiently large axial gap widths s_{ax}, the boundary layers are separated from each other and a co-rotating rigid-body vortex develops between them. [5, 10, 18, 20]

Normally, flow regime IV is present in water pumps [5, 10]. For the constellation of separated turbulent boundary layers, the radial velocities are always low compared to the circumferential velocities [5]. With regard to avoiding fiber entry into the back shroud cavity of a pump, this together with the above-mentioned flow pattern appears very convenient. It is tempting to assume that, due to the continuous and isolated radial-axial circulation, fibers contained in the main flow could not enter the back shroud cavity. And even if fibers were to be near parts within the back shroud cavity that are to be kept free of them, it could be expected that they are once more circulated away. However, in reality wastewater pumps have to be taken out of operation due to clogged back shroud cavities or destroyed mechanical seals.

2.2. Practice

In practice, the flow in the back shroud cavity differs considerably from the flow described for enclosed rotating disks. In both, annular and volute housings, the velocity and pressure distribution is rotationally asymmetrical at all operating points, causing the flow inside the back shroud cavity to be asymmetrical as well. Secondary flows through the back shroud cavity then occur as a result. [2, 5, 22, 23]

Furthermore, experiments and numerical simulations have shown that by actively dominating the flow through a suitable shroud geometry [22, 23] or by passively protecting the respective shroud cavity [24], asymmetric flow within front or back shroud cavity can, to a certain degree, be homogenized.

For instance, Bubelach [23] applied front vanes to the front shroud of a wastewater pump with a closed one-channel impeller. Compared to the flat disk-shaped front shroud configuration, the flow inside the front shroud cavity was less dependent of the circumferential pressure distribution in the annular housing.

Will et al. [22] numerically and experimentally investigated the flow inside the front as well as the back shroud cavity of a commercial standard pump with a single volute and a closed seven-channel impeller. Flow regime III was observed to prevail in the back shroud cavity due to low axial gap width s_{ax}. Viscous effects therefore had, to a certain degree, a homogenizing influence on the back shroud cavity flow.

Numerical and experimental investigations carried out by Knop et al. [24] showed that, in addition to the pressure distribution in the housing, the pressure distribution in the impeller eye can also affect the flow in the front shroud cavity. The pressure field in the impeller eye was homogenized by adapting the impeller geometry, which prevented further clogging of the one-channel wastewater impeller.

2.3. Housing Recesses

The extent to which the back shroud cavity is influenced by outer boundary conditions can be controlled by the design of the back shroud cavity, i.e. the design of the housing and the back shroud [5]. When the back shroud cavity is relatively open at the outer impeller diameter, the back shroud cavity flow is strongly coupled to the flow in the housing and the main flow behind the impeller outlet [5, 22]. In contrast, when recessing the rear housing wall in a way that the radial gap width s_r is small, whereas the degree of back shroud coverage c_{BS} is high, the back shroud cavity flow can be decoupled from outer boundary conditions to a large extent [5]. The degree of back shroud coverage c_{BS} is determined as follows, using the parameters shown in Fig. 1:

$$c_{BS} = \frac{d_{HR} - s_{ax}}{t_{BS}} \tag{1}$$

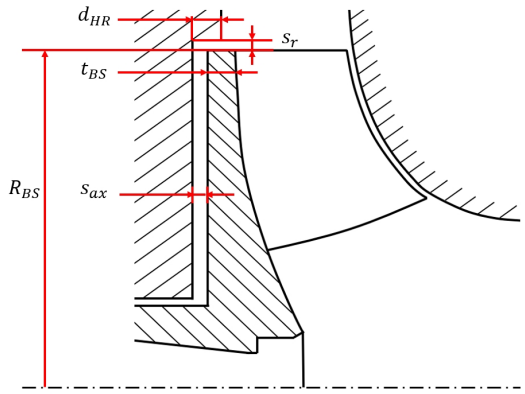

Figure 1. Back shroud cavity parameters

With regard to the fiber entry, it is therefore expected that the discussed local, centripetally directed secondary flows in particular lead to an increase in fiber entry and thus to a decrease in functionality in open and accordingly strongly coupled back shroud cavities. It is vice versa assumed that with increasing degree of back shroud coverage c_{BS} and decreasing radial gap width s_r, the back shroud cavity flow is increasingly decoupled from the external boundary conditions stated above, thus decreasing fiber entry. It is of special interest for the investigation presented to obtain information on both the effectiveness as well as the corresponding magnitude of the parameters back shroud coverage c_{BS} and radial gap width s_r. Increased radial thrust is to be expected for increasingly decoupled back shroud cavity designs, as pressure balancing secondary flows through the back shroud cavity are weakened [5].

3. EXPERIMENTAL INVESTIGATION

3.1. Investigated Pump

The dry-installed wastewater pump investigated has a semi-open two-channel impeller with a specific speed n_q and N_s at best efficiency point (Q100) of 58 min^{-1} and 3000 min^{-1}, respectively. Its outer diameter is 277 mm. The impeller is modified in a way that different back shroud geometries can be mounted. Therefore, the original back shroud geometry was turned off and subsequently featured threaded holes. The investigated pump has a volute housing and is driven by a 4-pole asynchronous motor. The rear housing wall is made of acrylic glass and hence fully transparent. It is furthermore equipped with threaded holes on different radii, so that the flat disk-shaped rear housing wall can be modified.

3.2. Test Rig

Figure 2 shows the open loop test rig operated for the experiments conducted. The water tank (WT) replicates a wastewater pumping station suction chamber. It has a capacity of 6 m^3 as well as fully transparent acrylic glass walls. During each test, artificial wastewater moves from the water tank through

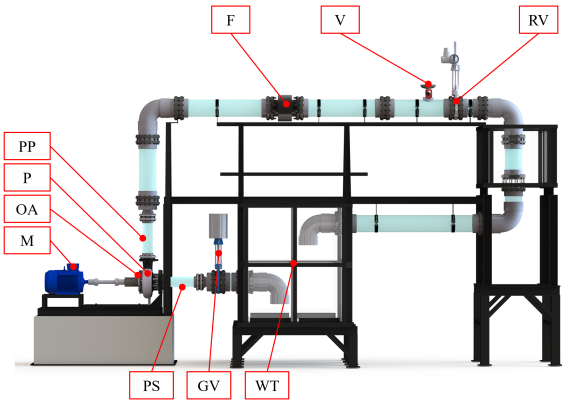

WT	water tank	OA	optical access
GV	gate valve	M	electric motor
PS	pressure measuring section (suction side)	F	flowmeter
PP	pressure measuring section (pressure side)	V	(de-) aeration valve
P	wastewater pump	RV	regulation valve

Figure 2. Test rig [15]

a DN 250 elbow pipe into the DN 150 suction line, where the static pressure upstream the pump is obtained (PS). From there, the artificial wastewater is transported through the test pump (P) and the DN150 discharge line, where the static pressure downstream the pump is measured (PP). From there, the artificial wastewater passes a shock diffuser and continues flowing through a magneto-inductive flowmeter (F). It subsequently passes a valve (V) installed for aeration as well as deaeration before passing the regulation valve (RV). Downstream, the artificial wastewater flows back into the water tank (WT).

3.3. Artificial Wastewater

To replicate fiber-laden wastewater, a defined quantity of microfiber rags is mixed with clear water in accordance with the standard DWA-A 120-2 [8] and other work investigating the functionality of wastewater pumps such as [9] or [12]. The *loading class* chosen corresponds to 25 rags per 1 m^3 of clear water, which complies with the lowest loading class defined in [8]. The total amount of microfiber rags thus corresponds to 150 per each of the tests conducted.

3.4. Housing Recess Configurations

Figure 1 shows the main parameters relevant for the housing recess configurations. The axial gap with s_{ax} was kept constant at 5 *mm*. This axial gap width was chosen due to the results of previous experiments [15] on the influence of the axial gap width s_{ax} between flat disk shaped back shroud and rear housing wall on fiber entry into the back shroud cavity of the same wastewater pump. The tests with axial gap widths s_{ax} of 1, 2, 3, 4 and 5 *mm* showed a general decrease in fiber entry with decreasing axial gap width. In order to assess the effectiveness of the recess configurations presented in this paper, it was decided to select the maximum gap width as a reference, at which the chance of fiber entry is high. Radial gap width s_r as well as degree of back shroud

Table 1. Housing recess configurations

Designation	c_{BS} [-]	s_r[mm]	S_r[-]
HR 0.8	0	8	0.0578
HR 50.8	0.5	8	0.0578
HR 100.8	1	8	0.0578
HR 0.2	0	2	0.0144
HR 50.2	0.5	2	0.0144
HR 100.2	1	2	0.0144

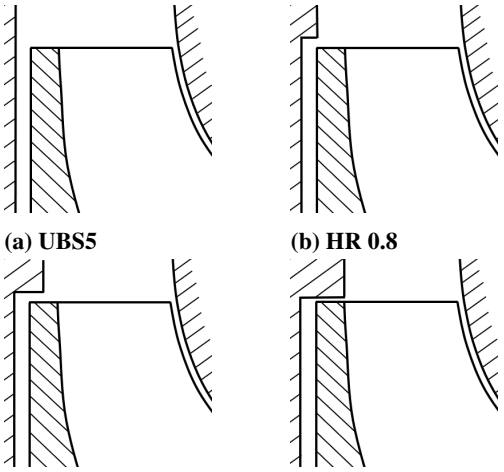

(a) UBS5 **(b) HR 0.8**

(c) HR 50.8 **(d) HR 100.2**

Figure 3. Selected configurations in comparison

coverage c_{BS} were varied throughout the tests. Table 1 provides an overview over the investigated housing recess geometries. Several of these configurations as well as the reference configuration UBS5 are illustrated in Fig. 3. The given designations correspond to the type of modification, the back shroud coverage c_{BS} and the radial gap width s_r. In order to easily compare the housing recess geometries presented with those in other pumps, it is also useful to specify the radial gap ratio as follows:

$$S_r = \frac{s_r}{R_{BS}} \tag{2}$$

The various configurations were implemented by screwing 3D printed polylactide rings onto the acrylic glass back wall, as shown for configuration HR 100.8 in Fig. 4.

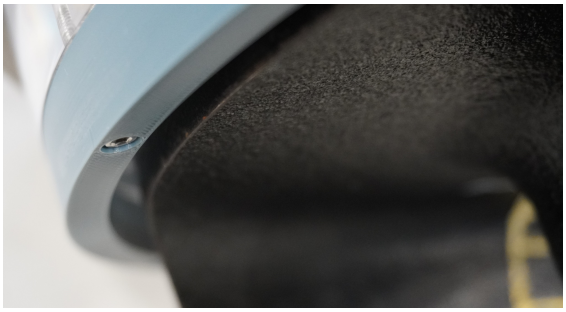

Figure 4. Radial gap of housing recess configuration HR 100.8

3.5. Test Procedure

For each configuration, three different operating points were investigated, one at part load (Q50), one at best efficiency point (Q100) and one at overload (Q120). For a corresponding configuration, three tests were performed per operating point. Each configuration was evaluated regarding the permanent dry fiber mass entry into the back shroud cavity after a test duration of 60 *min* after completion of the ramp-up process.

Prior to each test, reference values for head and electrical power were obtained for the flow rate of interest under clearwater conditions. The reference values are needed to monitor the operating behavior throughout each test as well as to determine any geometry-induced influence on both, operating behavior and aggregate efficiency. The latter is obtained as follows:

$$\eta_a = \frac{P_{hydr}}{P_{el}} = \frac{\rho g Q H}{P_{el}} \tag{3}$$

At the end of each test, the pump was switched off and the test rig was drained into a filtration system, where the fiber-laden water was prepared for the next test. The bearing bracket and the impeller were then removed. After taking the impeller off the shaft, possible fiber accumulations were collected and subsequently dried in a dehydrator until no more evaporation-induced weight loss was detectable. Table 2 provides an overview of the uncertainties of the measurement methods used.

Table 2. Measurement uncertainties

Quantity	Uncertainty
flow rate	± 0.2 % of value
differential pressure	± 0.05 *bar*
electrical power	± 1 % of value
mass	± 0.005 *g*

4. RESULTS

The configurations listed in Table 1 are evaluated below on the basis of the dry fiber mass entry into the back shroud cavity. Results for the reference configuration of equal back shroud geometry without housing recess *UBS5* obtained in [15] are used as a reference. In Fig. 5 and 7, the markers, upper bars and lower bars represent the mean, maximum and minimum values of dry fiber mass entry, respectively.

4.1. Radial Gap Width s_r of 8 mm

Figure 5 shows the results for the housing recess geometries with a radial gap width s_r of 8 *mm*. At part load Q50, no fiber entry into the back shroud cavity was detected for all configurations investigated.

At best efficiency point Q100, however, significant fiber entry into the back shroud cavity took place when testing configuration HR 0.8, as shown

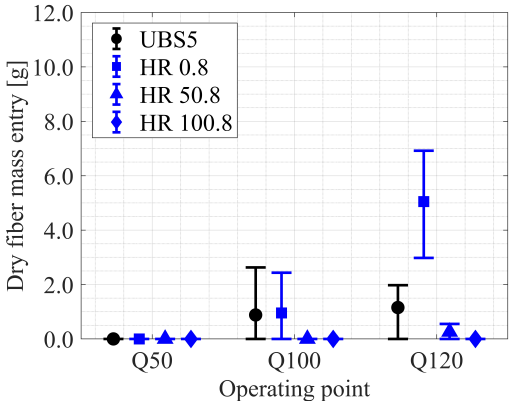

Figure 5. Dry fiber mass entry at s_r of 8 *mm*

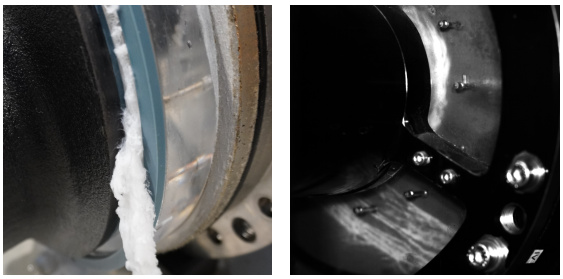

(a) best efficiency point **(b) overload**

Figure 6. Fiber accumulations observed when operating configuration HR 0.8

in Fig. 6a. For this configuration, which fully covers the back shroud cavity but not the back shroud, the fiber entry was quantitatively very similar to that of the recess-free reference configuration UBS5. In contrast, configurations HR 50.8 as well as HR 100.8 showed no fiber entry at best efficiency point, effectively reducing fiber entry into the back shroud cavity.

At overload operation Q120, fiber entry was distinctly increased by configuration HR 0.8. Compared to configuration UBS5, mean fiber entry more than quadrupled. As shown in Fig. 6b, once more fibers were observed to jam the passage to the back shroud cavity. In addition, fibers wound up on the rotating hub. With partial back shroud coverage c_{BS} of 0.5 in contrast, fiber entry was significantly reduced, as the mean value of 0.26 *g* corresponds to 22.5 % of the fiber entry registered for configuration UBS5 at this operating point. Configuration HR 100.8, due to its full back shroud coverage, eliminated any fiber entry at overload operation Q120.

4.2. Radial Gap Width s_r of 2 mm

For the housing recess geometries with a smaller radial gap width s_r of 2 *mm*, the operating point-dependent dry fiber mass entry is shown in Fig. 7.

With exception of configuration HR 50.2, none of the configurations examined at part load Q50 showed any significant fiber entry into the back shroud cavity. This is remarkable, since significant fiber entry into the back shroud cavity proved to be

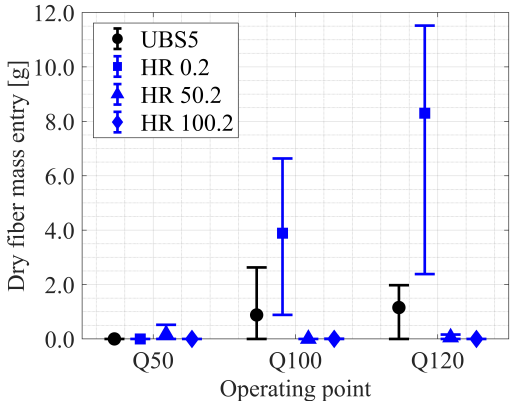

Figure 7. Dry fiber mass entry at s_r of 2 *mm*

rare for the investigated pump at part load. However, two of the three tests carried out with configuration HR 50.2 at part load were free of any fiber entry.

At best efficiency point Q100, HR 0.2 was found to be the only housing recess configuration with significant fiber entry into the back shroud cavity. In Fig. 8a fibers jammed in the passage to the back shroud cavity can be seen. Figure 8b shows the massive amount of fibers wound up on the hub after the same test at best efficiency point with a dry mass fiber entry of more than 6.6 g.

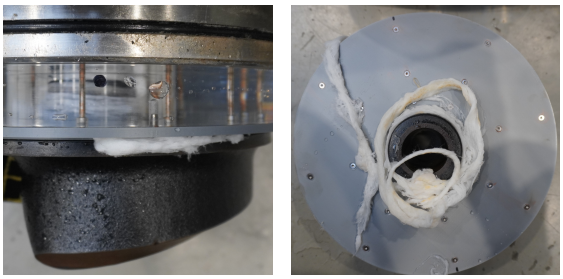

(a) jammed fibers **(b) wound up fibers**

Figure 8. Fiber accumulations after operating configuration HR 0.2 at best efficiency point

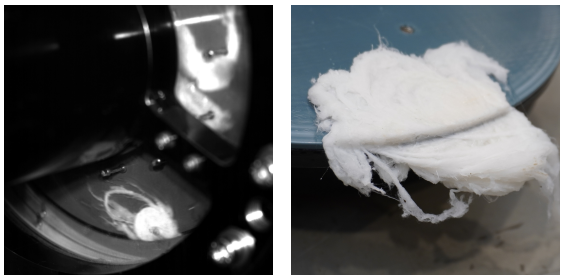

(a) during operation **(b) after operation**

Figure 9. Configuration HR 0.2 at overload

When operating the housing recess configurations with a radial gap width s_r of 2 *mm* at overload Q120, strongly increased fiber entry was detected for HR 0.2 once more. With a maximum value of 11.52 g for this configuration at this operating point, the largest dry fiber mass entry of the entire test series was determined. Again, fibers were seen to both wind up on the rotating hub and jam the passage to the back shroud cavity, as shown in Fig. 9a. As can be further seen in Fig. 9b, the fiber entry was so severe, that the back shroud as well as the recess geometry were damaged and had to be replaced. With a value of 0.16 g, maximum dry fiber mass entry was much less due to increased back shroud coverage c_{BS} but still considerable when operating housing recess configuration HR 0.5 at overload. It was again the configuration with the maximum back shroud coverage c_{BS}, that showed no fiber entry at overload.

4.3. Influence on Performance

In Fig. 10 it can be seen that fibers jamming the passage to the back shroud cavity were particularly evident when examining the recorded performance data, including electric power input P_{el}, hydraulic power output P_{hydr} as well as the resulting aggregate efficiency η_a. Reference values P_{el} and P_{hydr} obtained prior to this test corresponded to 12.45 kW and 8.06 kW, respectively. As can be seen in Fig. 10a, P_{el} increased to 12.89 kW by the end of the test due to the frictional torque caused by the jammed fibers, while P_{hydr} was reduced to 7.84 kW. Aggregate efficiency η_a was thus significantly reduced from 0.648 to 0.609. This influence on the performance data could only be determined for strong jamming of fibers accumulated in the passage to the back shroud cavity. In the case of minor fiber accumulations of this type as well as fibers wound up on the hub or the shaft, no such influence on the operating behavior was determined.

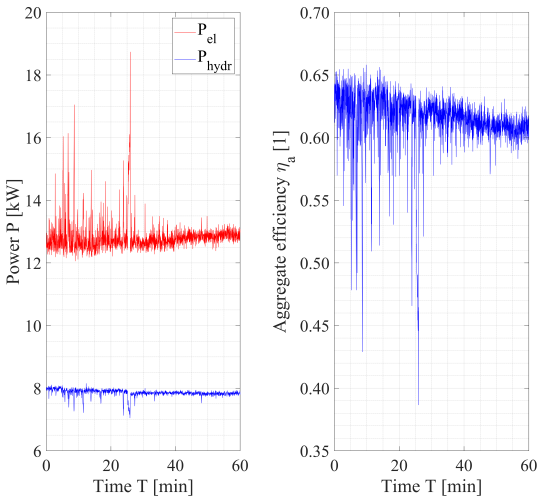

(a) power **(b) efficiency**

Figure 10. Performance data for configuration HR 0.2 at overload

4.4. Clear Water Efficiency Comparison

Measures to increase functionality are also to be evaluated on the basis of their influence on efficiency. Improving the clogging behavior of a wastewater pump often goes together with a reduction in efficiency. Figure 11 shows the aggregate efficiency η_a averaged over the three operating points for all housing recess configurations investigated as well as the recess-free reference configuration UBS5. It can be seen that the aggregate efficiency η_a for the introduced housing recess configurations is generally equal or higher compared to configuration UBS5. Furthermore, aggregate efficiency overall proved to increase with increasing degree of back shroud coverage c_{BS} and decreasing radial gap width s_r.

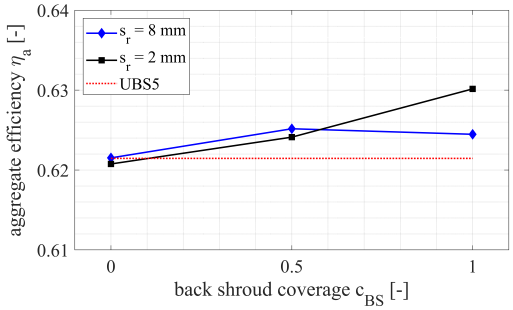

Figure 11. Operating point-averaged aggregate efficiency

4.5. Discussion

For the investigated pump and range of the parameters back shroud coverage c_{BS} and radial gap width s_r, the presented results lead to the finding that to prevent fiber entry into the back shroud cavity by decoupling back shroud cavity and housing using a suitable recess geometry, high back shroud coverage c_{BS} is to be preferred over small radial gap width s_r. This deduction is based on the fact that for all radial gap widths s_r investigated, the increase to moderate and to complete back shroud coverage c_{BS} generally led to a significant reduction and complete elimination of fiber entry, respectively. In contrast, for configurations with insufficient back shroud coverage c_{BS}, an increase in fiber entry with decreasing radial gap width s_r was evident.

As discussed in section 2.3, decoupling the back shroud cavity flow from the flow in the housing was expected to decrease fiber entry into the back shroud cavity. It was further elaborated, that the extent to which these flows are decoupled generally increases with increasing back shroud coverage c_{BS} and decreasing radial gap width s_r. These expectations have only proven to be valid for housing recess configurations in which the decoupling of the back shroud cavity flow was pursued by sufficiently large back shroud coverage c_{BS} and radial gap widths s_r that are not too small. However, this does not directly contradict the literature from which the expectations were derived, as the findings stated therein refer to clear water conditions without fibers or other solids. With only 2 *mm*, the minimum radial gap width s_r selected in this work may provide a significant decoupling of the back shroud cavity from external boundary conditions under clear water conditions. Despite this, however, this proved to result in an unfavorable passage to the back shroud cavity, which causes fiber accumulations to get jammed as well as prevents them from easily exiting the back shroud cavity.

In cases of severe jamming, electrical power input P_{el} was observed to increase, whereas hydraulic power output P_{hydr} was determined to decrease, thus decreasing aggregate efficiency η_a. In the case of minor jamming or fibers wound up on the hub or the shaft, no such influence was detected. Compared to the recess-free reference configuration, clearwater aggregate efficiency η_a of the housing recess configurations presented was equal or higher by up to nearly 0.01.

5. SUMMARY

Based on the literature discussed, potential influences of housing recesses on the back shroud cavity flow and the resulting fiber entry were derived. In order to determine the respective influence of the relevant parameters back shroud coverage c_{BS} and radial gap width s_r, suitable back shroud cavity configurations with housing recesses were designed. A test procedure to assess the functionality of these housing recess configurations was presented. The corresponding configurations were experimentally investigated and evaluated on the basis of dry fiber mass permanently accumulated in the back shroud cavity after pumping artificial wastewater for 60 *min*. The experiments conducted lead to the finding that fiber entry into the back shroud cavity is significantly reduced or completely eliminated as the back shroud coverage c_{BS} is increased. In contrast, an increase in fiber entry was determined when reducing the radial gap width s_r for configurations with insufficient back shroud coverage c_{BS}. Fibers were then frequently observed to jam the passage to the back shroud cavity, reducing aggregate efficiency η_a in severe cases. Fibers were also seen to wind up on the hub or the shaft. However, a related significant influence of this phenomenon on pump performance was not detected. The investigated housing recess geometries showed equal and, in case of partial or full back shroud coverage, increased aggregate efficiency η_a.

However, further knowledge about the prevailing flow within the back shroud cavity is to be determined numerically or experimentally. Since the results presented only apply to the investigated wastewater pump, it is of further interest to find out whether the findings apply to other pumps as well.

REFERENCES

[1] Gerlach, S., and Thamsen, P. U., 2017, “Cleaning Sequence Counters Clogging: A Quantit-

ative Assessment Under Real Operation Conditions of a Wastewater Pump", *Volume 1A, Symposia: Keynotes; Advances in Numerical Modeling for Turbomachinery Flow Optimization; Fluid Machinery; Industrial and Environmental Applications of Fluid Mechanics; Pumping Machinery*, American Society of Mechanical Engineers, Fluids Engineering Division Summer Meeting, p. V01AT05A001.

[2] Surek, D., 2014, *Pumpen für Abwasser- und Kläranlagen - Auslegung und Praxisbeispiele*, Springer Vieweg Wiesbaden, Wiesbaden.

[3] Mitchell, R.-L., 2019, "Causes, effects and solutions of operational problems in wastewater systems due to nonwoven wet wipes", *Environmental Science*.

[4] Hochstrat, I., 2024, "European nonwovens production decreased again", *FS Journal - Filtrieren und Separieren*.

[5] Gülich, J. F., 2020, *Kreiselpumpen - Handbuch für Entwicklung, Anlagenplanung und Betrieb*, Springer Vieweg, Heidelberg.

[6] Ren, Y., Zhao, L., Mo, X., Zheng, S., and Yang, Y., 2024, "Visualization investigation of the motion of rags in a double blades pump", *AIP Advances*, Vol. 14 (1), p. 015070.

[7] Nardone, R., and Flitney, B., 2006, "The effect of impeller back pump-out vanes on seal performance", *Sealing Technology*, Vol. 2006 (2), pp. 9–11.

[8] Deutsche Vereinigung für Wasserwirtschaft, A. u. A. e. V. D., 2022, *Arbeitsblatt DWA-A 120-2: Pumpsysteme außerhalb von Gebäuden – Teil 2: Pumpstationen und Drucksysteme*, DWA, Hennef.

[9] Beck, D., Brokhausen, F., and Thamsen, P. U., 2022, "Time-Resolved Measurements for the Detection of Clogging Mechanisms", *ASME 2022 Fluids Engineering Division Summer Meeting*.

[10] Wesche, W., 2016, *Radiale Kreiselpumpen: Berechnung und Konstruktion der Hydrodynamischen Komponenten*, VDI-Buch, Springer Vieweg, Berlin.

[11] Schindl, H., and Payer, H.-J., 2015, *Strömungsmaschinen. Band 1, Inkompressible Medien*, De Gruyter Oldenbourg, Munich ; Vienna, ISBN 3110343819.

[12] Pöhler, M., and Thamsen, P. U., 2019, "Mythos Kugeldurchgang – Aussage über Verstopfungsanfälligkeit bei Abwasserpumpen?", *WWT Wasserwirtschaft Wassertechnik*, Vol. 7 (8), pp. 12–17.

[13] Karassik, I. J., and McGuire, T., 1998, *Centrifugal Pumps*, Springer, New York.

[14] Schulz, H., 1977, *Die Pumpen*, Springer, Berlin/Heidelberg.

[15] Rinnert, T., and Thamsen, P. U., 2025, "Experimental Investigation of the Influence of the Axial Gap Width in the Back Shroud Cavity on the Clogging Behavior of a Wastewater Pump", *Submitted to Proceedings of the 16th European Turbomachinery Conference (ETC16)*.

[16] Rinnert, T., and Thamsen, P. U., 2025, "The Effect of Backward Curved Back Vanes and Back Channels on Fiber Entry Into the Back Shroud Cavity of a Wastewater Pump", *Submitted to Proceedings of the ASME 2025 Fluids Engineering Division Summer Meeting (FEDSM 2025)*.

[17] Pfleiderer, C., and Petermann, H., 2005, *Strömungsmaschinen*, Springer, Berlin.

[18] Schultz-Grunow, F., 1935, "Der Reibungswiderstand rotierender Scheiben in Gehäusen", *ZAMM - Zeitschrift für Angewandte Mathematik und Mechanik*, Vol. 15 (4), pp. 191–204.

[19] Ippen, A. T., 2022, "The Influence of Viscosity on Centrifugal-Pump Performance", *Transactions of the American Society of Mechanical Engineers*, Vol. 68 (8), pp. 823–838.

[20] Daily, J. W., and Nece, R. E., 1960, "Chamber Dimension Effects on Induced Flow and Frictional Resistance of Enclosed Rotating Disks", *Journal of Basic Engineering*, Vol. 82 (1), pp. 217–230.

[21] Nece, R. E., and Daily, J. W., 1960, "Roughness Effects on Frictional Resistance of Enclosed Rotating Disks", *Journal of Basic Engineering*, Vol. 82 (3), pp. 553–560.

[22] Will, B.-C., Benra, F.-K., and Dohmen, H.-J., 2012, "Investigation of the flow in the impeller side clearances of a centrifugal pump with volute casing", *Journal of Thermal Science*, Vol. 21, pp. 197–208.

[23] Bubelach, T., 2009, *Untersuchung der Radseitenraumströmung in einer Einschaufelrad-Abwasserpumpe*, Mensch und Buch Verlag, Berlin.

[24] Knop, M., Baack, T., Hohmeier, B., Di Brino, M., Petrak, G., Kamps, M., Dohmen, H.-J., and Benra, F.-K., 2022, "Erfolgreicher Kampf gegen die Verzopfung - Entwicklung, Bau und erste Betriebserfahrungen eines optimierten Laufrads für Schmutzwasserpumpen", *Korrespondenz Abwasser, Abfall*, Vol. 69, pp. 387–398.